ORIGINAL RESEARCH PAPER

A computational tool for the microstructure optimisation of a polymeric heart valve prosthesis

Authors

Serrani M[1], Brubert J[1], Stasiak J[1], De Gaetano F[2], Zaffora A[2], Costantino ML[2], Moggridge GD[1]

Author's affiliation

1- *Department of Chemical Engineering & Biotechnology*
University of Cambridge
Pembroke Street, Cambridge, CB23RA, UK

2- *Department of Chemistry Materials and Chemical Engineering "Giulio Natta"*
Politecnico di Milano,
Piazza Leonardo da Vinci 32, 20133 Milan, Italy

Corresponding author contact:

Marta Serrani
Department of Chemical Engineering & Biotechnology
University of Cambridge
Pembroke Street, Cambridge, CB23RA, UK
email: ms2214@cam.ac.uk

keywords: polymeric heart valve, heart valve prosthesis, computational modelling

Abstract

Styrene based block co-polymers are promising materials for the development of a polymeric heart valve prosthesis (PHV); the mechanical properties of these polymers can be tuned via the manufacturing process, orienting the cylindrical domains to achieve material anisotropy. The aim of this work is the development of a computational tool for the optimisation of the material microstructure in a new PHV intended for aortic valve replacement to enhance the mechanical performance of the device. An iterative procedure was implemented to orient the cylinders along the maximum principal stress direction of the leaflet. A numerical model of the leaflet was developed; the polymer mechanical behaviour was described by a hyperelastic anisotropic constitutive law. A custom routine was implemented to align the cylinders with the maximum

principal stress direction in the leaflet for each iteration. The study was focused on valve closure, since during this phase the fibrous structure of the leaflets must bear the greatest load. The optimal microstructure obtained by our procedure is characterised by mainly circumferential orientation of the cylinders within the valve leaflet. An increase in the radial strain and a decrease in the circumferential strain due to the microstructure optimisation was observed. Also, a decrease in the maximum value of the strain energy density was found in the case of optimised orientation; since the strain energy density is a widely used criterion to predict elastomer's lifetime, this result suggests a possible increase of the device durability if the polymer microstructure is optimised. The present method represents a valuable tool for the design of a new anisotropic PHV, allowing the investigation of different designs, materials and loading conditions.

Introduction

In the surgical treatment of aortic valve diseases, polymeric heart valve (PHV) prostheses have the potential to combine the hemodynamics and the low thrombogenicity of biological prostheses, with the durability of mechanical prostheses. Yet, no PHV is currently used in clinical practice; several PHV prototypes, mainly composed of polyurethane-based materials, have been developed since the 1960's (Akutsu *et al.*, 1959) but, despite their promising short-term outcomes (Mackay *et al.*, 1996; Bernacca *et al.*, 2001; Ghanbari *et al.*, 2009; Rahmani *et al.*, 2012; Claiborne *et al.*, 2013), none have shown satisfactory long-term reliability, due primarily to calcification and tearing of the leaflets (Bernacca *et al.*, 1995, 1997; Bezuidenhout *et al.*, 2015; Kheradvar *et al.*, 2015). The achievement of an adequate device lifetime remains the main challenge in the development of a clinically viable polymeric prosthesis. In this context, the geometry and material design are critical to obtaining optimal mechanical performance of the device.

In the literature, many authors have highlighted the importance of material anisotropy on aortic valves' behaviour. In fact, natural valve leaflets are characterized by the presence of collagen bundles basically oriented in the circumferential direction, embedded in an elastic matrix (Vesely, 1998; Balguid *et al.*, 2007; Sacks *et al.*, 2009; Rock *et al.*, 2014). As a consequence of this particular architecture, the leaflet circumferential stiffness is significantly larger than the radial stiffness (about 15 MPa vs 2 MPa (Mavrilas & Missirlis, 1991; Balguid *et al.*, 2007)). Even if the mechanisms underlying this tissue arrangement is not completely understood, it surely influences the valve mechanical behaviour and failure mechanism (Burriesci *et al.*, 1999; Billiar & Sacks, 2000*a*; Stella & Sacks, 2007; Sacks *et al.*, 2009; Saleeb *et al.*, 2012; Loerakker *et al.*, 2013). The anisotropic tissue structure allows the valve to open easily due to the low resistance of collagen fibres to bending and increases the material stiffness and strength during valve closure. Some authors have tried to mimic the anisotropic structure of the natural valve in PHV prostheses, mainly by using reinforcement fibres in the leaflets (Hart *et al.*, 1998; Cacciola *et al.*, 2000; Liu *et al.*, 2007); however, a clear improvement in prosthesis lifetime with such devices has not been proven, and none of these devices reached a clinical evaluation stage.

Recently, different polymers characterized by good biostability and biocompatibility have been developed as possible materials for the development of PHVs (Puskas & Chen, 2004); among them, *block co-polymers* represent a promising class of material (Ranade *et al.*, 2005; Pinchuk *et al.*, 2008). In particular, the good biocompatibility and the suitable mechanical properties of *styrene based block co-polymers* for application in heart valve prostheses have been demonstrated (Gallocher *et al.*, 2006; El Fray *et al.*, 2006; Claiborne *et al.*, 2011, 2013; Bezuidenhout *et al.*,

2015; Brubert *et al.*, 2016). Further, our group has recently shown the possibility of tuning the microstructure and, consequently, the mechanical properties of this type of polymer by compression and slow injection moulding: the investigation of thin moulded films of poly(styrene-*block*-isoprene-*block*-styrene), a block co-polymer characterized by a cylindrical morphology, revealed a layered orientation of the cylinders which depends on the conditions during the manufacturing process (i.e. flow rate and temperature) (Stasiak *et al.*, 2014, 2015); this layered structure leads to a strong anisotropy of the material, as demonstrated by mechanical tests of material samples. Thus, following a mechanism similar to the native valve where the collagen bundles sustain most of the stress, the optimisation of the cylinders' orientation in the valve leaflets could enhance the long-term performance of the PHV, making this class of material an excellent candidate for the development of a new polymeric aortic valve prosthesis. We have already tested some PHV prototypes made of polystyrene-containing block co-polymer in continuous and pulsatile flow conditions, as prescribed by the ISO 5840 Standard. A custom-made pulse duplicator was used to test the prototypes at different flow rate and frequency conditions; pressure and flow signals were recorded and pressure drops, effective orifice area (EOA), and regurgitant volume were computed. All the tested PHVs met the requirements defined by the ISO 5840 Standard (EOA > 1 cm^2 and regurgitant volume < 10% of the stroke volume.), indicating good device hydrodynamics under the prescribed conditions (De Gaetano *et al.*, 2015a, 2015b). However, these valves were not optimised in terms of material microstructure and determining the optimum cylinders' orientation of the PHV is one of the main challenges to solve in the development of a new anisotropic valve. The aim of this work was to develop a computational tool for the optimisation of the PHV microstructure. The basic idea was to orient the polymer microstructure in the leaflets along the maximum principal stress direction, to allow the cylinders to act as reinforcements in the most stressed direction. The optimisation procedure herein presented has general validity, and could easily be applied to different type of valves, materials and loading conditions.

Methods

A computational model of the PHV leaflet was developed; the simulations' outcomes allowed the identification of the maximum principal stress directions in the leaflet, while a custom routine was implemented to optimize the material microstructure. Only one leaflet was considered due to the valve's geometric periodicity (120°); the presence of the other leaflets and of a rigid stent was

taken into account by applying suitable boundary conditions. The study was focused on valve closure, since during this phase the fibrous structure of the leaflets must bear the greatest load. For the sake of clarity the description of the optimisation procedure and of the finite element (FE) model implementation is presented below in different sections: (1) Leaflet geometry, (2) Material description, (3) Material microstructure optimisation and (4) Boundary and other simulation conditions.

(1) Leaflet geometry

A 3D model of the PHV leaflet was designed by means of the CAD (*Computer Aided Design*) software Rhinoceros 5 (Rhinoceros, Robert McNeel & Associates). The valve design, and particularly the leaflet shape, is fundamental to ensuring correct valve opening and closing under physiological blood pressure. For this reason, the aortic valve geometry has been investigated by different authors (Swanson & Clark, 1974; Thubrikar, 1990; Labrosse *et al.*, 2006). In the present work, a tri-leaflet symmetric valve with constant leaflet thickness and identical material properties in each leaflet was assumed. The leaflet shape consists of a central spherical region where the circular free edge is extended tangentially to connect the leaflet with the valve stent; the commissural edge is cut in a cylindrical shape (Figure 1). The valve internal diameter was set at 23 mm, the leaflet height at 11 mm, while the leaflet thickness was constant and equal to 0.3 mm.

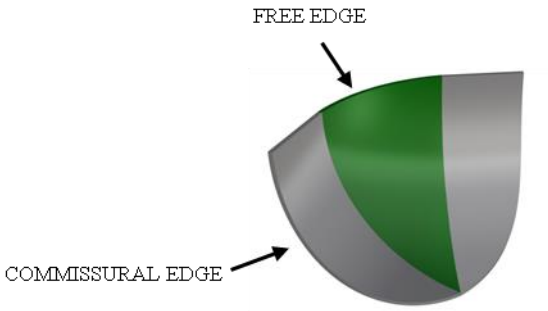

Figure 1. CAD design of the valve leaflet; the spherical belly region is coloured in green. Geometrical parameters: valve diameter=23 mm; leaflet height=11 mm; leaflet thickness=0.3 mm.

(2) Material description

The mechanical behaviour of block co-polymers is characterized by a non-linear stress-strain relationship which is strongly dependent on the microdomain architecture (Pakula *et al.*, 1985; Stasiak *et al.*, 2009). In fact, block co-polymers with cylindrical domains can show either isotropic or anisotropic behaviour, depending on the orientation of the material (Stasiak *et al.*, 2009). The mechanical behaviour of block co-polymers can be well described by a hyperelastic constitutive law, where the material response is determined by a strain energy function ψ. Under the hypothesis

of material incompressibility (namely, volume ratio in the deformation process $J = det(\boldsymbol{F}) = 1$), the strain energy can be written as

$$\psi = \psi(\boldsymbol{C}) - p(J - 1) \quad \text{(Eq.1)}$$

where $\boldsymbol{C}$ is the right Cauchy-Green tensor and p is the hydrostatic pressure.
The strain energy can be further divided into an isotropic and an anisotropic contribution to take into account the material's anisotropic microstructure by considering

$$\psi(\boldsymbol{C}) = \psi_{iso}(\boldsymbol{C}) + \psi_{aniso}(\boldsymbol{C})\,. \quad \text{(Eq.2)}$$

For the isotropic part of the potential, a Mooney-Rivlin stress-strain relationship was assumed; in terms of the principal invariants of $\boldsymbol{C}$ it can be written as

$$\psi_{iso} = \psi_{iso}(I_1, I_2) = c_1(I_1 - 3) + c_2(I_2 - 3) \quad \text{(Eq.3)}$$

where c_1 and c_2 are material parameters to be identified.
Finally, the anisotropic contribution of ψ has been defined as (Perotti *et al.*, 2013)

$$\psi_{aniso} = \psi_{aniso}(I_4) = k_4 log^2\sqrt{I_4} \quad \text{(Eq.4)}$$

where k_4 is a parameter to be determined from mechanical tests of the material. I_4 is a pseudo-invariant of $\boldsymbol{C}$ which takes account of the cylinders' orientation by the unit vector $\boldsymbol{a}$

$$I_4 = \boldsymbol{a_0} \cdot \boldsymbol{C a_0} = \boldsymbol{a^T} \cdot \boldsymbol{a}\,; \quad \text{(Eq.5)}$$

in Eq.5, $\boldsymbol{a_0}$ defines the cylinders' direction in the undeformed configuration, while $\boldsymbol{a}$ defines the cylinders' direction in the deformed configuration. In fact, I_4 measures the square of the stretch along the cylinders' direction.
Summarizing, the proposed strain energy function has the form

$$\psi = c_1(I_1 - 3) + c_2(I_2 - 3) + k_4 log^2\sqrt{I_4} - p(J - 1)\,; \quad \text{(Eq.6)}$$

this material constitutive law was implemented in the software by using the UANISOHYPER subroutine. The stress is computed from the strain energy by derivation with respect to the right Cauchy-Green tensor $\boldsymbol{C}$ as

$$\boldsymbol{\sigma} = 2J^{-1}\boldsymbol{F}\frac{\partial\psi(\boldsymbol{C})}{\partial\boldsymbol{C}}\boldsymbol{F^T} \qquad \text{(Eq. 7)}$$

which, for the constitutive law defined in Eq.6, gives

$$\boldsymbol{\sigma} = 2\left[\left(\frac{\partial\psi}{\partial I_1} + I_1\frac{\partial\psi}{\partial I_2}\right)\boldsymbol{b} - \frac{\partial\psi}{\partial I_2}\boldsymbol{b}^2 + \frac{\partial\psi}{\partial I_4}\boldsymbol{a}\otimes\boldsymbol{a}\right] - p\boldsymbol{I} \qquad \text{(Eq. 8)}$$

where $\boldsymbol{b}$ is the left Cauhy-Green tensor (for a detailed description of hyperelastic material modelling refer to Holzapfel (2000)).

In the case of isotropic material, the anisotropic contribution was dropped; thus, three material parameters have to be identified for the anisotropic case (c_1, c_2 and k_4) and two parameters for the isotropic case (c_1 and c_2). In both cases the parameters were optimized using the non linear least square algorithm to match data from experimental mechanical tests, by means of a custom MATLAB (MATLAB, The MathWorks, Inc.) routine (Figure 2).

Experimental protocol

Uniaxial tensile tests (Texture Analyser, Stable Microsystems, UK) were performed on dogbone samples (length=100 mm; width=4 mm; thickness=0.7 mm) up to 70% elongation at a speed of 1 mm/s, according to the ASTM standard D882. About 100 preconditioning cycles were performed in order to reach a reproducible stress-strain behaviour between two subsequent cycles. Both the isotropic and anisotropic materials were tested; for the anisotropic case two cylinder orientations were considered: parallel and perpendicular to the principle strain direction. A minimum of three samples were tested for each material. The isotropic samples were obtained by solvent casting, whilst the anisotropic samples were fabricated via compression moulding at 160°C, as previously described by Stasiak *et al.* (2010). The specific block co-polymer used to fabricate the samples was poly(styrene-block-ethylene/propylene-block-styrene), a linear block co-polymer characterised by a cylinder length of 200 - 500 nm. The results of the experimental tests and the optimised material model are shown in Figure 2; the optimized material parameters for the isotropic and anisotropic materials are presented in Table 1.

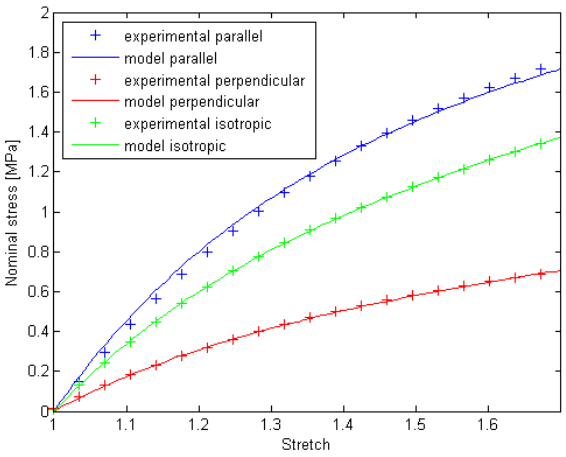

Figure 2. Experimental and modelled stress-strain relationship for the isotropic and the anisotropic case. For the anisotropic case, both the direction parallel and perpendicular to the principle strain direction are presented.

Table 1. Optimised material parameters

	c_1 [MPa]	c_2 [MPa]	k_4 [MPa]
Anisotropic	0.15	0.18	1.62
Isotropic	0.3	0.36	\

(3) Material microstructure optimisation

The cylinders' orientation was set in the material model by defining the vector $\boldsymbol{a_0}$, which describes the material microstructure in the reference configuration (Eq.5). The microstructure vector $\boldsymbol{a_0}$ can be set in both the Cartesian ($\boldsymbol{e}$) and material ($\tilde{\boldsymbol{e}}$) reference systems, the two systems being related by the relationship

$$\tilde{\boldsymbol{e}} = \boldsymbol{Q}\boldsymbol{e}\,, \quad \boldsymbol{e} = \boldsymbol{Q}^{\boldsymbol{T}}\tilde{\boldsymbol{e}} \qquad \text{(Eq.7)}$$

where $\boldsymbol{Q}$ is an orthogonal tensor and is referred to as the transformation matrix.

The orientation of $\boldsymbol{a_0}$ was optimized by an iterative procedure which, starting from an initial guess, aligns the cylinders' direction with the maximum principal stress direction. For this purpose, a custom MATLAB routine was implemented. The routine defines the cylinders orientation' in the nth iteration based on the results of the $(n\text{-}1)$th iteration in terms of maximum principal stress directions; each iteration consists of a FE simulation aimed at finding the maximum principal stress

direction in the leaflet from the Cauchy stress tensor (see par. 4 for a description of the FE model implementation).

Specifically, for each element of the leaflet mesh a different local reference system was defined; this local system was rotated between the (*n-1*)th and the *n*th iteration to align one axis of the new reference system (the axis along which the microstructure vector $\boldsymbol{a_0}$ is oriented) with the maximum principal stress direction obtained in the previous iteration. Thus, calling $\boldsymbol{r_0}$ the microstructure vector at the (*n-1*)th iteration, the vector $\boldsymbol{a_0}$ at the *n*th iteration was obtained by

$$\boldsymbol{a_0} = \boldsymbol{R_0 r_0} \qquad \text{(Eq.8)}$$

where $\boldsymbol{R_0}$ represents the rotation matrix, defined from the angle between the vector $\boldsymbol{r_0}$ and the maximum principal stress direction in the (*n-1*)th iteration (Figure 3). Finally, the routine transforms $\boldsymbol{a_0}$ such that it refers to the undeformed configuration, in order to find the cylinders' orientation at the beginning of the next iteration.

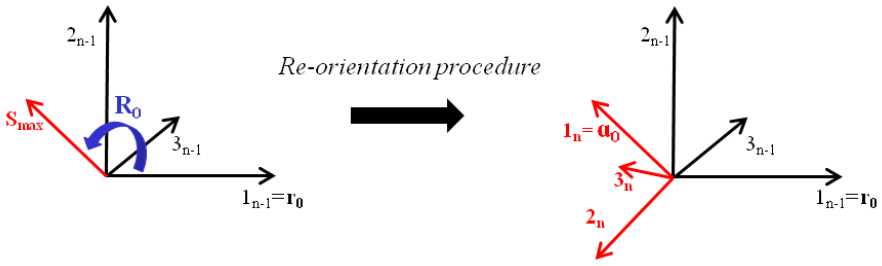

Figure 3. Schematic representation of the cylinders' re-orientation procedure: for each element, the first axis of the reference system in the (*n-1*)th iteration is rotated via the matrix R_0, which superimposes this axis with the maximum principal stress direction of iteration *n-1*. Thus, the new reference system to be used in the *n*th iteration is obtained.

The optimisation process ends when the percentage of the element's local reference systems which are rotated more than 5° between two subsequent iterations is less than 1%. Different starting orientations were set to ensure the robustness of the re-orientation procedure, indicating that the starting orientation did not affect the optimised microstructure; hence, for sake of simplicity a starting orientation in the *x* global axis direction was chosen.

(4) Boundary and other simulation conditions

A rigid valve stent was assumed; to simulate the effect of the rigid stent on the leaflet dynamics no displacements at the commissural surface were permitted. To mimic the presence of the other

two leaflets of the valve, two rigid planes were defined and a frictionless contact was implemented between each of these planes and the ventricular surface of the leaflet. Preliminary simulations comparing the one and the three leaflets case ensured the suitability of this boundary condition in the presence of a rigid stent. These simulations showed how for the case of a flexible stent the twisting in the middle of leaflets during closing can influence the mechanical response of the valve; however, no twisting has been found in the case of a rigid stent, thus the modelling of a single leaflet was adequate for the aim of the present study. A uniform pressure load was applied on the aortic surface of the leaflet; different backpressures have been modelled in the range specified by the ISO Standard 5840 as operational environment for an aortic valve prosthesis (95-185 mmHg). Since the results of the optimisation procedure are similar in all the simulated cases, for the sake of brevity the only case of pressure equal to 135 mmHg is presented hereinafter. A quasi-static loading condition was assumed (Luo *et al.*, 2003; Sun, 2005; Haj-Ali *et al.*, 2008); the nonlinear implicit FE algorithm provided by ABAQUS was used to solve the numerical problem. The leaflet geometry was discretised in 15330 hexahedral linear elements to perform the FE analyses. Specifically, three elements were placed across the leaflet's thickness to correctly model the structure bending. Simulations with an increasing number of elements up to about 60000 elements were performed to ensure the independence of the results from the mesh size.

Results and Discussion

The result of the optimisation process is shown in Figure 4. Starting from the initial configuration where the cylinders are aligned along the *x* global axis (identified as the baseline), the optimal microstructure obtained by our procedure shows primarily circumferential orientation within the valve leaflet, except for a region close to the commissural edge where the orientation is more radial. No discontinuities are present in the cylinders' orientation across the thickness, since the maximum stress direction is quite constant over the three layers in which the geometry was discretised (see Boundary conditions section). Three iterative steps were necessary to reach this optimum material microstructure according to the criterion described in the Methods section; however, as highlighted in Figure 5, most of the cylinders' re-orientation is completed after the first iteration. Interestingly, the optimised architecture just described reproduces quite well the structure of a native aortic valve leaflet (Billiar & Sacks, 2000*a*), where the collagen bundles exhibit a pattern which is similar to the optimum distribution of cylinders in the PHV (Figure 4). This evidence further confirms, as highlighted by other studies (Boerboom *et al.*, 2003; Driessen

et al., 2003), that the natural leaflet is well adapted by remodelling during growth to withstand the pressure load exerted by the blood during valve closure. It is worth noting that in our case the maximum stress direction is aligned with the maximum strain direction; thus, a strain-driven optimisation criterion, such as that hypothesised by Driessen *et al.* (2003) for the native aortic valve would lead to the same result in terms of material microstructure.

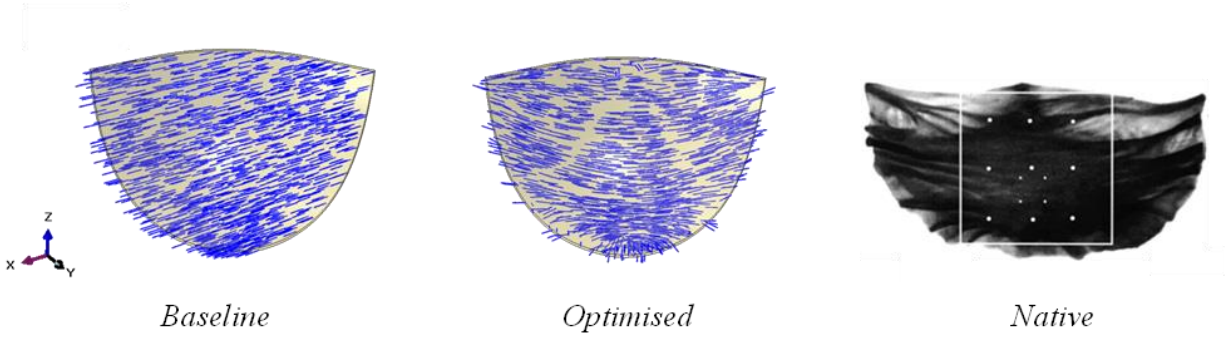

Figure 4. Cylinder orientation within the leaflet at the beginning (baseline, left) and at the end (optimised, middle) of the optimisation process. Right: collagen fibre architecture in a native porcine aortic valve (Billiar & Sacks, 2000*a*).

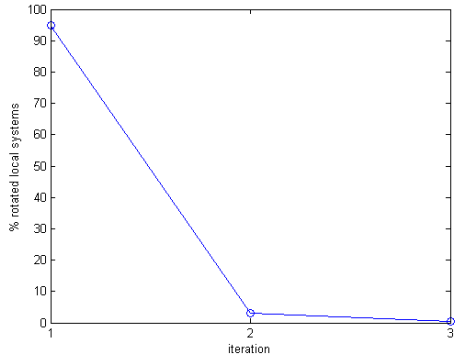

Figure 5. Percentage of rotated local systems in the model for each iteration. After three iterations the cylinder orientation changes in fewer than 1% of the total elements of the leaflet.

In order to study in more detail the effect of the material microstructure on the leaflet mechanics, the stress and strain distributions in the PHV leaflet for both optimised and isotropic material were analysed (Figure 6).

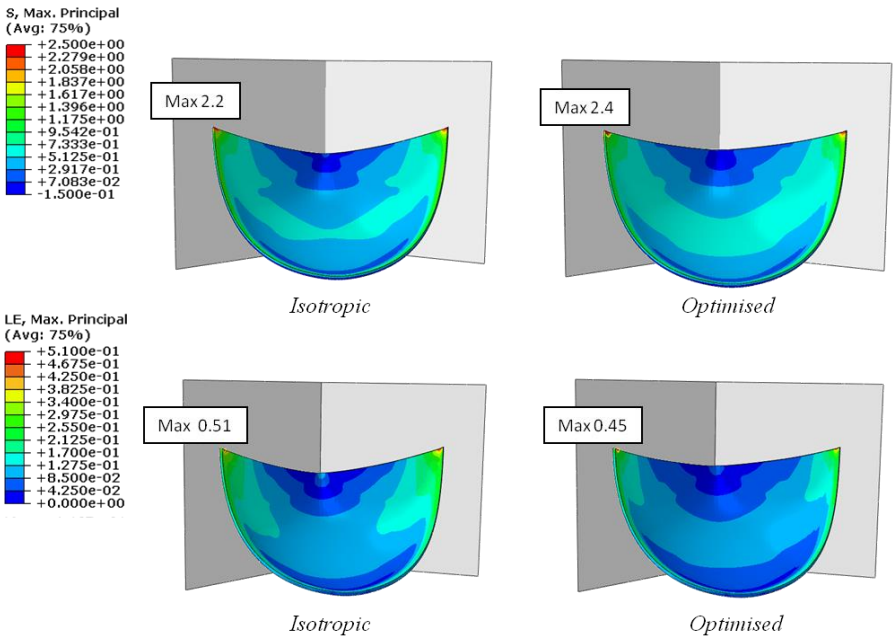

Figure 6. Maximum principal stress (top) and maximum principal logarithmic strain (bottom) distributions in the leaflet in case of isotropic and anisotropic material.

The comparison between optimised and isotropic material demonstrates a similar stress distribution with the maximum stress location at the top of the commissural edge (Figure 6, top); the maximum stress is about 8% greater when the material is optimally oriented compared to the non-oriented material. This result is in agreement with other published studies, where the material anisotropy contributes to an increase in the maximum stress present in the leaflet, because of the higher stiffness in the loading direction (Hart *et al.*, 1998; Li *et al.*, 2001; Luo *et al.*, 2003). However, in Li *et al.* (2001) and Luo *et al.* (2003) a change of the maximum stress location, from the top of the commissures to a point along the commissural edge, was also reported when an anisotropic leaflet material was considered. This difference to our results could be due to several factors, since the aforementioned studies were focused on porcine heart valves characterised by a different geometry, material properties and fibers orientation and distribution, to those used in this study.

As expected, the strain pattern shows an inverse trend (Figure 6, bottom): the optimised leaflet is characterised by a smaller maximum principal strain when compared to the isotropic material. Also, due to the material's mechanical behaviour, the difference in the maximum strain is larger than for the stress: the maximum strain is about 14% lower for optimised cylinder orientation than isotropic material.

In accordance to observations by Li *et al.* (2001), the macroscopic effect of the decrease in maximum strain is a reduction in the vertical displacement of the central point of the free edge, which is equal to 2.1 mm in the anisotropic case and 2.8 mm in the isotropic case.

However, the material stiffening in the maximum stress direction due to the cylinders' orientation doesn't affect the valve macroscopic closing: the coaptation area between the leaflets decreases of only 2% when the material is oriented compared to the isotropic case.
Further, the circumferential and radial strain were analysed (Figure 7).

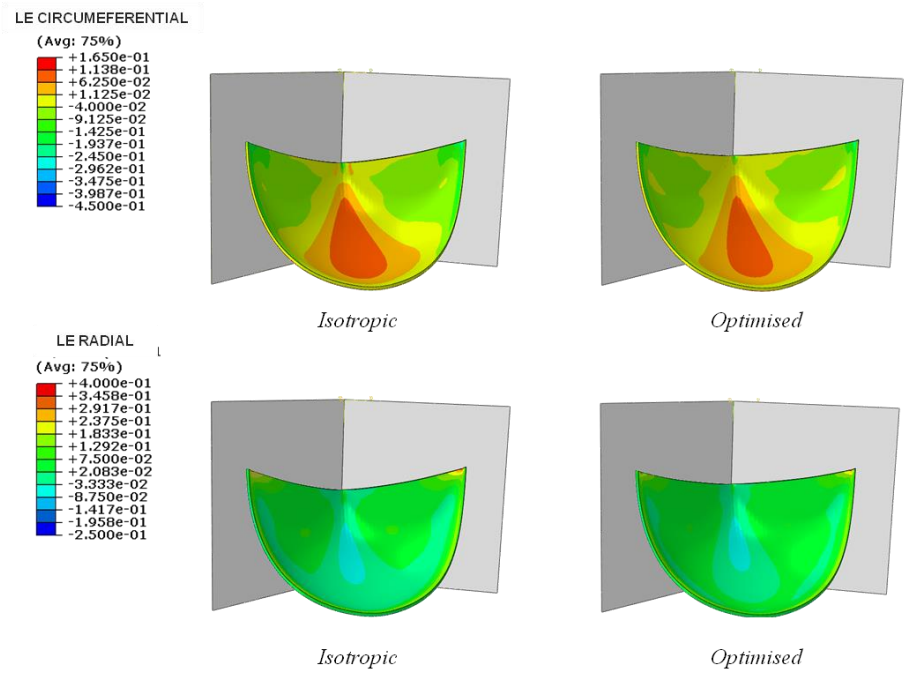

Figure 7. Circumferential (top) and radial (bottom) logarithmic strain in the isotropic and optimised cases.

The optimised microstructure leads to a smaller circumferential strain and a higher radial strain than those found in an isotropic valve, in accordance with the studies of Billiar & Sacks (2000*a*, 2000*b*) and Martin & Sun (2012) on the native valve, which highlighted how the natural tissue is mainly stretched in the radial direction due to the collagen fibres organisation.
A similar result was also obtained by Loerakker *et al.* (2013) with a model of tissue engineered heart valves, where a larger radial and smaller circumferential strain were found with an increased material anisotropy.
Hence, the results presented so far mainly show that an optimised polymer microstructure can enhance the material response to the pressure load, in fact mimicking the native valve's mechanical behaviour. However this data, while promising, does not in itself clarify whether an improvement in the fatigue life of the valve prosthesis will be achieved by properly controlling the polymer microstructure.

In the literature, different criteria have been proposed to predict elastomer's lifetime under cyclic loading; among them, the strain energy density is one of the most widely used parameters to investigate the fatigue behaviour of rubbers (Zarrin-Ghalami & Fatemi, 2012, 2013). Thus, to better understand the effect of the cylinders' orientation on the valve lifetime, the strain energy density was calculated for all the elements of the valve leaflet at the maximum applied pressure for the isotropic and anisotropic materials (Figure 8). For comparison purpose, the result for the baseline configuration is also shown (Figure 8); even if the baseline structure does not have any physical meaning, as it only represents the starting point of the optimisation procedure, it can be useful to understand the effect of a possible "accidental" material orientation due to an uncontrolled manufacturing process.

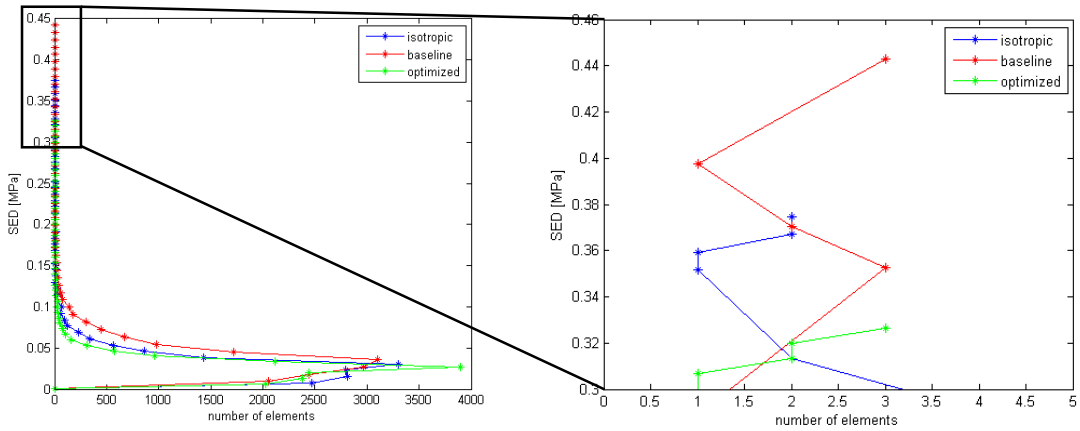

Figure 8. Strain Energy Density calculated for all the leaflet elements for isotropic and anisotropic cases. For the anisotropic material, both the baseline and the optimised configuration are presented.

The results show a decrease of about the 14% of the maximum value of the strain energy density when the material microstructure is optimised. Assuming that the valve failure mechanism is more likely to be initiated at points of high strain energy density, this finding suggests an improved long-term mechanical response for an optimised valve compared to an isotropic valve. Also, this result highlights the negative effect of a non optimised oriented material microstructure, since the baseline configuration exhibits the highest value of strain energy density among the analysed configurations (+25% when compared to the optimised case).

Conclusions

In this work a computation tool for the optimisation of a new polymeric aortic valve prosthesis made of styrene based block co-polymers is presented. An optimisation procedure was developed to align the cylindrical domains along the maximum stress direction, thus mimicking the effect of the collagen bundles in the native valve. As for the natural valve, the optimisation of the leaflet

microstructure is responsible for a reduction in the circumferential strain and an increase in the maximum stress. Further, the material stiffening along the most stressed direction doesn't negatively affect the valve regurgitation, as demonstrated by the leaflets' coaptation area which is almost the same in the case of isotropic or optimised microstructure. As in the native valve, the opening shouldn't be significantly influenced by the material orientation either, due to the very small resistance of the cylinders to the leaflet bending.

Furthermore, when the material is properly oriented, the maximum strain energy density is reduced, suggesting an improvement in the prosthesis' lifetime; however, experimental fatigue tests are required to confirm the validity of this result. The presented method can be of great value for the development of a reliable polymeric heart valve, in which valve geometry and material properties must be simultaneously optimised.

We have already demonstrated the possibility of orienting the material microstructure in compression and injection moulded flat samples (Stasiak et al., 2009; Stasiak et al. 2014). Also, we have fabricated compression moulded valves that showed acceptable hydrodynamic behaviour; although, in these valves, the material microstructure wasn't optimised. Based on the results of the present work, we have fabricated injection moulded valves with the aim of controlling the cylinders' orientation by the polymer flow during processing. The first results are encouraging, since a mainly circumferential orientation of the cylinders has been obtained in the leaflets. In this context, the model can also be used to predict the influence of small defects on the prosthesis behaviour, giving important indications about the valve manufacturing.

Some assumptions were made in the implementation of the computational model. Firstly, the viscoelastic properties of the polymer were neglected; although loading-unloading cycles performed on the material have shown only limited hysteresis and sensitivity to strain rate, progressive creep of the polymer chains during stretching could influence the mechanical response of anisotropic samples. Also, the material characterisation was obtained via uniaxial tensile tests; however, due to the polymer anisotropy and the valve loading conditions, biaxial tests would lead to more accurate results in terms of mechanical response of the material. Further, the solvent cast method ensures a random planar polymer chain distribution (namely a transverse isotropy), but some degree of anisotropy is still to be expected in the off-plane direction. Furthermore, a perfect alignment of the cylinders along the specified direction was considered, while some tests (Stasiak *et al*, 2010) highlighted a dispersion of the cylinders around the main orientation which could influence the mechanical behaviour of the material. Finally, only the closing phase was considered, since during this phase the fibres must bear the maximum load; the simulation of the valve opening will give further indications for the material optimisation and leaflet thickness. Despite these

limitations, the present model represents an extremely valuable tool for the design of any anisotropic valve, since each feature of the numerical model can be easily modified to understand the optimum material microstructure for different geometries, materials and boundary conditions.

The authors disclose that no financial and personal relationships with other people or organisations inappropriately influenced this work.

Acknowledgements

The authors thank the British Heart Foundation for financial support for this work under Grant NH/11/4/29059 and SP/15/5/31548.

Akutsu T, Dreyer B & Kolff WJ (1959). Polyurethane artificial heart valves in animals. *J Appl Physiol* **14,** 1045–1048.

Balguid A, Rubbens MP, Mol A, Bank R a, Bogers AJJC, van Kats JP, de Mol B a JM, Baaijens FPT & Bouten CVC (2007). The role of collagen cross-links in biomechanical behavior of human aortic heart valve leaflets--relevance for tissue engineering. *Tissue Eng* **13,** 1501–1511.

Bernacca GM, Mackay TG & Wilkinson R (1995). Calcification and fatigue failure in a polyurethane heart valve. *Biomaterials* **16,** 279–285.

Bernacca GM, Mackay TG, Wilkinson R & Wheatley DJ (1997). Polyurethane heart valves : Fatigue failure , calcification , and polyurethane structure. *J Biomed Mater Res* **34,** 371–379.

Bernacca GM, Straub I & Wheatley DJ (2001). Mechanical and morphological study of biostable polyurethane heart valve leaflets explanted from sheep. *J Biomed Mater Res*.

Bezuidenhout D, Williams DF & Zilla P (2015). Polymeric heart valves for surgical implantation, catheter-based technologies and heart assist devices. *Biomaterials* **36,** 6–25.

Billiar KL & Sacks MS (2000*a*). Biaxial Mechanical Properties of the Natural and Glutaraldehyde Treated Aortic Valve Cusp — Part I : Experimental Results. *J Biomech Eng* **122,** 23–30.

Billiar KL & Sacks MS (2000*b*). Biaxial Mechanical Properties of the Native and Glutaraldehyde-Treated Aortic Valve Cusp : Part II — A Structural Constitutive. *J Biomech Eng* **122,** 327–335.

Boerboom R, Driessen NJB, Bouten CVC, Huyghe JM & Baaijens FPT (2003). Finite Element Model of Mechanically Induced Collagen Fiber Synthesis and Degradation in the Aortic Valve. *Ann Biomed Eng* **31,** 1040–1053.

Brubert J, Krajewski S, Wendel HP, Nair S, Stasiak J & Moggridge GD (2016). Hemocompatibility of styrenic block copolymers for use in prosthetic heart valves. *J Mater Sci Mater Med* **27**, 1-12.

Burriesci G, Howard IC & Patterson EA (1999). Influence of anisotropy on the mechanical behaviour of bioprosthetic heart valves. *J Med Eng Technol* **23,** 203–215.

Cacciola G, Peters GWM & Baaijens FPT (2000). A synthetic fiber-reinforced stentless heart valve. *J Biomech* **33,** 653–658.

Claiborne TE, Girdhar G, Gallocher-Lowe S, Sheriff J, Kato YP, Pinchuk L, Schoephoerster RT, Jesty J & Bluestein D (2011). Thrombogenic potential of Innovia polymer valves versus Carpentier-Edwards Perimount Magna aortic bioprosthetic valves. *ASAIO J* **57,** 26–31.

Claiborne TE, Sheriff J, Kuetting M, Steinseifer U, Slepian MJ & Bluestein D (2013). In vitro evaluation of a novel hemodynamically optimized trileaflet polymeric prosthetic heart valve. *J Biomech Eng* **135,** 021021–021027.

Driessen N, Boerboom R, Huyghe JM, Bouten CV & Baaijens FP (2003). Computational Analyses of Mechanically Induced Collagen Fiber Remodeling in the Aortic Heart Valve. *J Biomech Eng* **125,** 549.

El Fray M, Prowans P, Puskas JE & Altstädt V (2006). Biocompatibility and fatigue properties of polystyrene-polyisobutylene-polystyrene, an emerging thermoplastic elastomeric biomaterial. *Biomacromolecules* **7,** 844–850.

De Gaetano F, Bagnoli P, Zaffora A, Pandolfi A, Serrani M, Brubert J, Stasiak J, Moggridge GD & Costantino ML (2015*a*). A newly developed tri-leaflet polymeric heart valve prosthesis. *J Mech Med Biol* **15,** 1540009.

De Gaetano F, Serrani M, Bagnoli P, Brubert J, StasiakJ, Moggridge GD, Costantino ML (2015*b*) Fluid Dynamic Performances of a new polymeric heart valve prototype (Poli-Valve) tested under Continuous and Pulsatile Flow Conditions. *Int J Artif Organs* **38,** 600-606.

Gallocher SL, Aguirre AF, Kasyanov V, Pinchuk L & Schoephoerster RT (2006). A Novel Polymer for Potential Use in a Trileaflet Heart Valve. *J Biomed Mater Res Part B Appl Biomater* **79B,** 325–334.

Ghanbari H, Viatge H, Kidane AG, Burriesci G, Tavakoli M & Seifalian AM (2009). Polymeric heart valves: new materials, emerging hopes. *Trends Biotechnol* **27,** 359–367.

Haj-Ali R, Dasi LP, Kim H-S, Choi J, Leo HW & Yoganathan AP (2008). Structural simulations of prosthetic tri-leaflet aortic heart valves. *J Biomech* **41,** 1510–1519.

Hart J De, Cacciola G, Schreurs PJG & Peters GWM (1998). A three-dimensional analysis of a fibre-reinforced aortic valve prosthesis. *J Biomech* **31,** 629–638.

Kheradvar A, Groves EM, Dasi LP, Alavi SH, Tranquillo R, Grande-Allen KJ, Simmons C a., Griffith B, Falahatpisheh A, Goergen CJ, Mofrad MRK, Baaijens F, Little SH & Canic S (2015). Emerging Trends in Heart Valve Engineering: Part I. Solutions for Future. *Ann Biomed Eng* **43,** 833–843.

Labrosse MR, Beller CJ, Robicsek F & Thubrikar MJ (2006). Geometric modeling of functional trileaflet aortic valves: development and clinical applications. *J Biomech* **39,** 2665–2672.

Li J, Luo XY & Kuang ZB (2001). A nonlinear anisotropic model for porcine aortic heart valves. *J Biomech* **34,** 1279–1289.

Liu Y, Kasyanov V & Schoephoerster RT (2007). Effect of fiber orientation on the stress distribution within a leaflet of a polymer composite heart valve in the closed position. *J Biomech* **40,** 1099–1106.

Loerakker S, Argento G, Oomens CWJ & Baaijens FPT (2013). Effects of valve geometry and tissue anisotropy on the radial stretch and coaptation area of tissue-engineered heart valves. *J Biomech* **46,** 1792–1800.

Luo XY, Li WG & Li J (2003). Geometrical Stress-Reducing Factors in the Anisotropic Porcine Heart Valves. *J Biomech Eng* **125,** 735.

Mackay TG, Wheatley DJ, Bernacca, Fisher AC & Hindlet CS (1996). New polyurethane heart valve prosthesis : design , manufacture and evaluation. *Biomaterials* **17,** 1857–1863.

Martin C & Sun W (2012). Biomechanical characterization of aortic valve tissue in humans and common animal models. *J Biomed Mater Res - Part A* **100 A,** 1591–1599.

Mavrilas D & Missirlis Y (1991). An approach to the optimization of preparation of bioprosthetic heart valves. *J Biomech* **24,** 331–339.

Pakula T, Saijo K, Kawai H & Hashimoto T (1985). Deformation behavior of styrene-butadiene-styrene triblock copolymer with cylindrical morphology. *Macromolecules* **18,** 1294–1302.

Perotti LE, Deiterding R, Inaba K, Shepherd J & Ortiz M (2013). Elastic response of water-filled fiber composite tubes under shock wave loading. *Int J Solids Struct* **50,** 473–486.

Pinchuk L, Wilson GJ, Barry JJ, Schoephoerster RT, Parel J-M & Kennedy JP (2008). Medical applications of poly(styrene-block-isobutylene-block-styrene) ("SIBS"). *Biomaterials* **29,** 448–460.

Puskas JE & Chen Y (2004). Biomedical application of commercial polymyers and novel polyisobutylene-based thermoplastic elastomers for soft tissue replacement. *Biomacromolecules* **5,** 1141–1154.

Rahmani B, Tzamtzis S, Ghanbari H, Burriesci G & Seifalian AM (2012). Manufacturing and hydrodynamic assessment of a novel aortic valve made of a new nanocomposite polymer. *J Biomech* **45,** 1205–1211.

Ranade S V., Richard RE & Helmus MN (2005). Styrenic block copolymers for biomaterial and drug delivery applications. *Acta Biomater* **1,** 137–144.

Rock C a, Han L & Doehring TC (2014). Complex collagen fiber and membrane morphologies of the whole porcine aortic valve. *PLoS One* **9,** e86087.

Sacks MS, David Merryman W & Schmidt DE (2009). On the biomechanics of heart valve function. *J Biomech* **42,** 1804–1824.

Saleeb AF, Kumar A & Thomas VS (2012). The important roles of tissue anisotropy and tissue-to-tissue contact on the dynamical behavior of a symmetric tri-leaflet valve during multiple cardiac pressure cycles. *Med Eng Phys* **35,** 23–35.

Stasiak J, Brubert J, Serrani M, Nair S, de Gaetano F, Costantino ML & Moggridge GD (2014). A bio-inspired microstructure induced by slow injection moulding of cylindrical block copolymers. *Soft Matter* **10,** 6077–6086.

Stasiak J, Brubert J, Serrani M, Talhat a., De Gaetano F, Costantino ML & Moggridge GD (2015). Structural changes of block copolymers with bi-modal orientation under fast cyclical stretching as observed by synchrotron SAXS. *Soft Matter* **11,** 3271–3278.

Stasiak J, Squires AM, Castelletto V, Hamley IW & Moggridge GD (2009). Effect of stretching on the structure of cylinder- and sphere-forming styrene-isoprene-styrene block copolymers. *Macromolecules* **42,** 5256–5265.

Stasiak J, Moggridge GD, Zaffora A, Pandolfi A, Costantino ML (2010). Engineering orientation in block copolymers for application to prosthetic heart valves. *Funct Mat Lett* **3**, 249-252.

Stella J a & Sacks MS (2007). On the biaxial mechanical properties of the layers of the aortic valve leaflet. *J Biomech Eng* **129,** 757–766.

Sun W (2005). Simulated Bioprosthetic Heart Valve Deformation under Quasi-Static Loading. *J Biomech Eng* **127,** 905.

Swanson WM & Clark RE (1974). Dimensions and Geometric Relationships of the Human Aortic Value as a Function of Pressure. *Circ Res* **35,** 871–882.

Vesely I (1998). The role of elastin in aortic valve mechanics. *J Biomech* **31,** 115–123.

Zaffora A (2011). Computational method for the design of innovative materials for heart valve prostheses. PhD thesis, Politecnico di Milano.

Zarrin-Ghalami T & Fatemi A (2012). Material deformation and fatigue behavior characterization for elastomeric component life predictions. *Polym Eng Sci* **52,** 1795–1805.

Zarrin-Ghalami T & Fatemi A (2013). Multiaxial fatigue and life prediction of elastomeric components. *Int J Fatigue* **55,** 92–101.